AIP | Applied Physics Letters

Primary and secondary droplet and charge transmission characteristics of desorption electro-flow focusing ionization

Thomas P. Forbes, Tim M. Brewer, and Greg Gillen

Citation: Appl. Phys. Lett. **102**, 214102 (2013); doi: 10.1063/1.4807789
View online: http://dx.doi.org/10.1063/1.4807789
View Table of Contents: http://apl.aip.org/resource/1/APPLAB/v102/i21
Published by the American Institute of Physics.

Primary and secondary droplet and charge transmission characteristics of desorption electro-flow focusing ionization

Thomas P. Forbes,[a] Tim M. Brewer, and Greg Gillen
Material Measurement Laboratory, National Institute of Standards and Technology, Gaithersburg, Maryland 20899, USA

(Received 14 March 2013; accepted 9 May 2013; published online 28 May 2013)

We present the investigation of droplet charging and charge transmission characteristics of an electro-flow focusing nozzle for desorption-based ambient ionization mass spectrometry. The electro-flow focusing geometry utilizes a concentrically flowing gas to focus a charged solvent stream through a small orifice, generating a steady liquid jet and charged droplet stream that impinges and ionizes the analyte and surface. Transmitted current measurements and a scaling analysis were incorporated to decouple analyte desorption and ionization from secondary droplet charging and to identify the regimes of operation, secondary droplet charge transport characteristics, and parameters limiting transmitted charge relevant for ambient ionization mass spectrometry.
[http://dx.doi.org/10.1063/1.4807789]

The identification and analysis of analytes on solid surfaces has broad significance to the military, law enforcement, transportation authorities, and first responders for forensic applications and the detection of narcotics and chemical, explosive, and biological threats. Trace detection systems incorporate a range of techniques, including immunoassays,[1] Raman spectroscopy,[2] ion mobility spectrometry (IMS),[3,4] and the focus of this Letter, ambient pressure ionization mass spectrometry (API-MS).[5,6] Reviews summarizing ambient and desorption-based ionization techniques,[7,8] most notably, desorption electrospray ionization (DESI),[5,6,9–11] can be found in the literature.

In this Letter, we investigate the current carried by primary and secondary droplets from an electro-flow focusing (EFF)[12–14] nozzle as they pertain to its use as a desorption-based ion source for mass spectrometric analysis of analytes on surfaces without the need for sample preparation, pretreatment, or separation. The electro-flow focusing ion source was characterized with transmitted current measurements to decouple the droplet charging and analyte solvation and ionization processes. In conjunction with a scaling analysis, these measurements defined regimes of operation, identified optimal conditions for secondary droplet charging, and exhibited the fundamental relationship between electro-flow focusing parameters and substrate material properties. This framework provides insight into the MS response, enabling rapid optimization of experimental parameters, i.e., fluid properties and operational conditions. With the established transmitted current framework, electro-flow focusing for desorption ionization mass spectrometry demonstrated intense analyte signals and high signal-to-noise ratio for focusing gas pressures and jet/droplet charging potentials nearly an order of magnitude less than the traditional desorption electrospray ionization technique.[5,6,9–11]

Figure 1 schematically represents the geometry of the electro-Flow Focusing® nebulizer (Ingeniatrics Tecnologías, Sevilla, Spain) with a 150 μm capillary inner diameter, 100 μm capillary-to-orifice distance, and 100 μm exit orifice diameter. The electro-flow focusing ion source was developed around the "flow focusing" (FF) technique originally developed by Gañán-Calvo.[12] Flow focusing incorporates a concentric gas stream to focus the solvent into a high velocity jet, emanating through a small orifice. The unique configuration and the fundamental physics of the flow focusing phenomenon allow for both high spatial resolution flow focusing and broad sampling flow blurring modes of operation.[12] In addition, the electro-flow focusing embodiment has the distinctive capability of operating in a purely mechanical flow focusing regime, purely electrospraying regime, or at the electro-flow focusing transition between the two. The flow regime and electrohydrodynamic spraying mode are a function of the fluid properties, e.g., density, conductivity, and surface tension, and operation conditions, e.g., gas pressure, fluid flow rate, and applied potential.[13,14]

The electro-flow focusing ion source generates primary charged solvent droplets that are sprayed onto a surface of interest (Figure 1). The high velocity primary microdroplets enhance solvation and ionization of the analyte molecules, while facilitating the ejection of secondary droplets toward the MS inlet. We performed an initial investigation of the secondary droplet current generated by electro-flow focusing

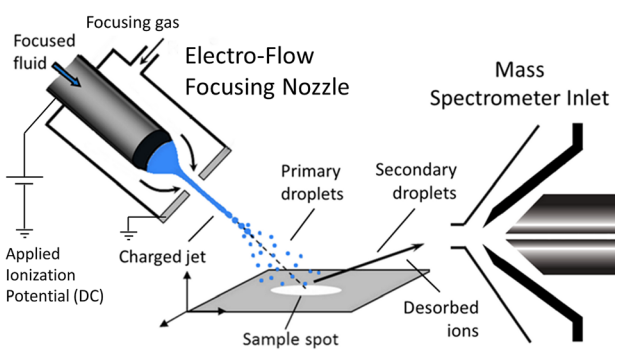

FIG. 1. Schematic representation of the electro-flow focusing ionization desorption-based ion source for mass spectrometry.

[a]Author to whom correspondence should be addressed. Electronic mail: thomas.forbes@nist.gov

in a surface sampling configuration, decoupled from the analyte desorption and ionization phenomena. For these current measurements, the vertical collecting electrode replaced the mass spectrometer inlet displayed in Figure 1. Charged drops were produced by applying a DC potential (High Voltage Power Supply, PS350, Stanford Research Systems, Sunnyvale, CA) to a metallic fitting on the source directly in contact with the spray solution and grounding the orifice plate (Figure 1). The current produced by the "splashing" of primary charged droplets off of the intermediate surface, generating secondary droplets impinging onto the collecting electrode was measured with a grounded picoammeter (Keithley Instruments Inc., model 485 picoammeter; Cleveland, OH). Additional current measurements were also taken at the electro-flow focusing orifice plate. The total electric current carried by the liquid jet was defined as the sum of the current discharging at the orifice plate and the current emitted from the electro-flow focusing source, measured at the collecting electrode.[14] However, the emitted current, and specifically the emitted current carried by the secondary droplets, remains the focus of this investigation.

To investigate the emitted current, we collapsed the experimental data using the scaling analysis and dimensionless parameters previously derived to characterize the electro-flow focusing atomization process.[14] This analysis also allowed us to identify the fundamental relationship between system parameters, enable rapid optimization of experimental parameters, and gain insight into their effect on the MS response. The analysis was based on an approximated one-dimensional analytical model of the underlying electrohydrodynamics equations, including the steady Navier-Stokes equations and interfacial stress boundary conditions (Maxwell and viscous stress tensors). The in-depth derivation of the model and dimensionless parameters has been described in detail elsewhere.[14] As defined in the literature,[14,15] the appropriate scales for the current carried by an electrospraying jet (I_{es}) and the voltage at the transition to electrospray (V_{es}) are $I_{es} \sim (\gamma\sigma Q)^{1/2}$ and $V_{es} \sim (\gamma\sigma\rho^2/\varepsilon_o^4)^{1/6} Q^{1/2}$, respectively. Here, γ is the focused fluid surface tension, σ is the fluid conductivity, ρ is the fluid density, ε_o is the permittivity of free space, and Q is the volumetric flow rate of the fluid.

Figure 2 displays the deflected secondary current as a function of the applied voltage for a few fluid flow rates and (69 ± 3) kPa (approximately 10 psi) focusing gas pressure, scaled by the theoretical electrospray current, I_{es}, and transition voltage, V_{es}, respectively. It is important to note that the voltages reported here are the applied potentials and not the liquid voltage at the capillary tip. The reported potentials do not account for the voltage drop due to the liquid line electrical resistance between the potential application point and capillary tip. As intuitively expected and demonstrated in the literature, the current increased with increasing potential and increasing solvent flow rate. In the range of applied potentials considered, the measured secondary droplet current impacting the collecting electrode asymptotically approached a maximum value that was dependent on the fluid flow rate. In addition, the scaled applied voltage at which the asymptotic behavior began decreased with increasing flow rate. The orifice and total currents monotonically increased with increasing applied potential in the range investigated here (see supplementary information, Figure S1[16]). As discussed in detail in the literature,[14] the highly charged droplets generated by the high electric fields experienced in the region between the liquid capillary and emitting orifice were in principle discharged by the grounded orifice as they passed. It was hypothesized that this discharging process was due to corona discharge effects as the local electric field surpasses the gas dielectric strength and gas ionization as small highly charged droplets evaporate.[14] Therefore, for equivalent system parameters, as the flow rate increased, the effective distance between the focused fluid and orifice exit decreased. As demonstrated in Figure 2, the decrease in distance between the charged liquid and grounded orifice resulted in lower voltages necessary for the onset of discharge effects of the electrified jet and emitted current saturation, $V/V_{es} \approx 10$, $V/V_{es} \approx 8$, and $V/V_{es} \approx 6$, for 3, 5, and 8 μL/min, respectively.

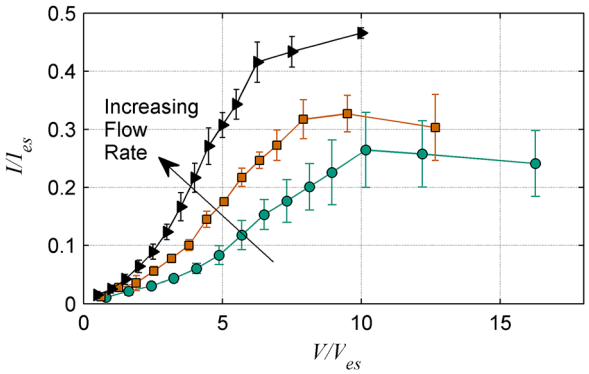

FIG. 2. Experimentally measured dimensionless secondary droplet current as a function of dimensionless voltage for a 50% (volume fraction) methanol solution in water sprayed onto a glass slide as a function of applied potential for a 50° angle, 70 kPa focusing gas pressure, and 3 μL/min (-●-), 5 μL/min (-■-), and 8 μL/min (-▶-) flow rates. Data points and uncertainty expressed as the average values and standard uncertainties (represented by the standard deviation), respectively, for steady state currents obtained from 3 to 5 experiments.

As introduced above, electro-flow focusing occurs at the transition between the purely mechanical "flow focusing" regime and the purely electrical "electrospray" regime. Figure 3(a) demonstrates the measured current of secondary droplets deflected off of a glass surface, the current discharged at orifice, and the total current. When these values were compared to the directly measured current of the primary droplets (Figure 3(b)), i.e., no intermediate deflection, the total electro-flow focusing current at high applied potentials, approached the theoretical electrospray current ($I_{total} \leq I_{es}$). Figure 3 also displays the empirical relationship between the total electrified jet current and applied potential from Gañán-Calvo *et al.*[14] The discrepancies between that study and the present study were dominated by the differences in device geometry, i.e., Gañán-Calvo *et al.*[14] investigated an electro-flow focusing device with a smaller capillary-to-orifice distance and considered higher flow rates. Both of these geometrical aspects would lead to a reduction in the characteristic length of the electric field resulting in jet/droplet discharge, and therefore comparable electric field strengths at reduced scaled applied voltage as demonstrated in Figures 2 and 3. In addition, Gañán-Calvo *et al.*[14] included a correction factor for the voltage drop between the application point and capillary tip, further adding to the discrepancy in scaled voltages between studies.

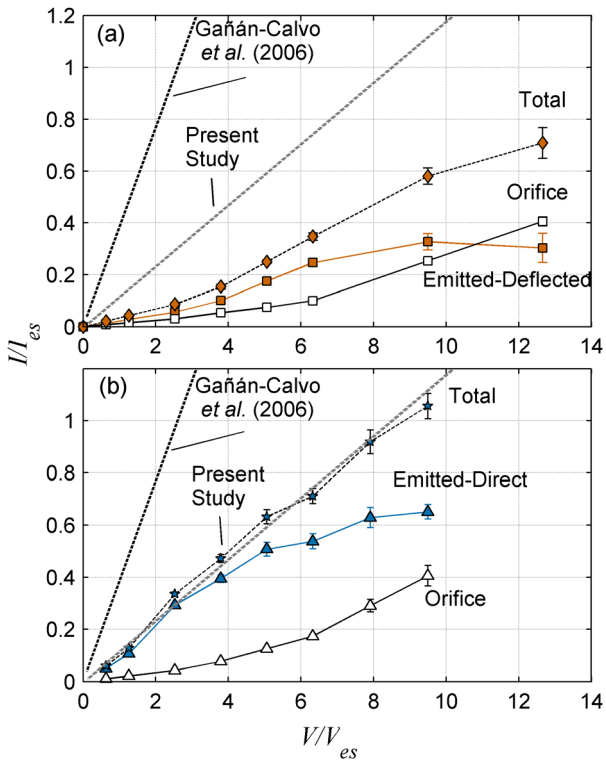

FIG. 3. Experimentally measured dimensionless secondary droplet current as a function of dimensionless voltage for a 50% (volume fraction) methanol solution in water as a function of applied potential for a 50° angle, 70 kPa focusing gas pressure, and 5 μL/min flow rate. Measured orifice current, collecting electrode current, and total electrified jet current for (a) secondary droplet deflection off of a glass slide (-□-, -■-, -◆-) and (b) primary droplet spraying directly (-△-,-▲-,-⋆-), respectively. Black and gray dotted lines represent the empirical relationship between total jet current and applied voltage from Gañán-Calvo *et al.*[14] and the present study, respectively. Data points and uncertainty expressed as the average values and standard uncertainties (represented by the standard deviation), respectively, for steady state currents obtained from 3 to 5 experiments.

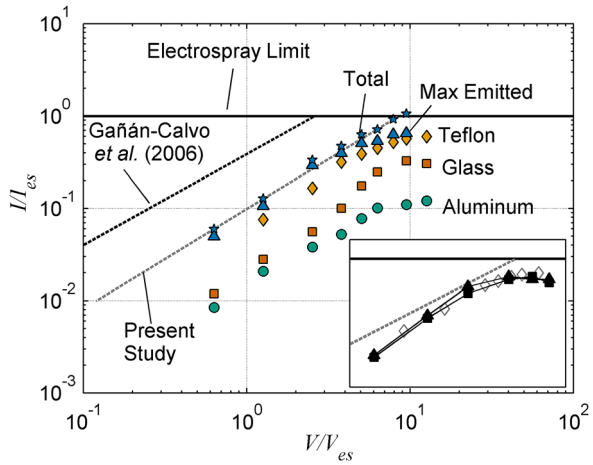

FIG. 4. Experimentally measured dimensionless secondary droplet current deflected off of an (●) aluminum, (■) glass, and (◆) PTFE (Teflon®) substrate, as a function of dimensionless voltage for a 50% (volume fraction) methanol solution in water as a function of applied potential for a 50° angle, 70 kPa focusing gas pressure, and 5 μL/min flow rate. Total electrified jet current (⋆) and emitted primary droplet current (▲) also displayed. Black and gray dotted lines represent the empirical relationship between total jet current and applied voltage from Gañán-Calvo *et al.*[14] and the present study, respectively. Solid line at $I/I_{es} = 1$ represents the transition to electrospraying. Inset: normalized mass spectrometric total ion current for positive mode MS (cocaine analysis, -■-) and negative mode MS (RDX analysis, -▲-) as a function of dimensionless voltage. Gray open diamond data points represent dimensionless deflected current from main figure for the PTFE substrate.

While the total current approached that of electrospraying, the useful emitted current that generated secondary droplets was limited by the corona discharge and gas ionization effects experienced due to the electro-flow focusing source geometry and operational physics.[14] Figure 3 also clearly demonstrates the reduction in the emitted current carried by the primary droplet and the deflected secondary droplet streams. For desorption ionization mass spectrometry, we focus on maximizing the secondary droplet current for efficient analyte ionization. Figure 4 displays the deflected secondary droplet current for a number of substrate materials, including polytetrafluoroethylene (PTFE, Teflon®), glass, and aluminum. While a portion of the reduction in emitted current magnitude demonstrated in Figure 3 can be attributed to current losses from drops that were not successfully transported from the nozzle to the collecting electrode, Figure 4 points to the transport of charge and the inherent capacitive charging of the intermediate substrate[17] as the main contributing factors. The secondary current as a function of applied potential and the maximum achievable secondary current (asymptotic saturation value) both decrease for more conducting and more wetting interrogated surfaces (Figure 4). Not surprisingly, for highly conductive substrates, e.g., aluminum, the charge carried by the primary droplet stream can dissipate on almost instantaneous time scales, which led to drastic reductions in the charge carried by secondary droplets. Table I provides material properties and charge relaxation time scales, $t_{relax} \sim \varepsilon_r \varepsilon_o / \sigma_{cond}$, for the substrates considered in this study, where σ_{cond} and ε_r are the electrical conductivity and relative permittivity, respectively, of the material. The charge relaxation time scale approached zero for the conducting aluminum, was on the order of minutes for glass, and effectively infinite for PTFE (Table I). The PTFE substrate demonstrated secondary droplet current measurements that approached the maximum achievable emitted current of the primary droplet stream. Figure 4 also exhibits a nearly constant scaled applied voltage $(V/V_{es} \approx 8)$ for the onset of discharge effects at the grounded orifice and emitted current saturation, across the range of intermediate surfaces interrogated, all at equivalent flow rates. This further verified that the applied voltage for achieving the asymptotic current was a function of the electro-flow focusing device geometry and flow rate (effectively the characteristic length scale for the discharging electric field) and the maximum achievable current was a function of both the flow rate and intermediate substrate material properties.

Finally, we ionized and detected cyclotrimethylenetrinitramine (RDX) and cocaine (see supplementary information, Figures S2 and S3[16]) off of Teflon coated wells on a standard Prosolia Omni Slide™ with the electro-flow focusing source

TABLE I. Material properties and charge relaxation time scales.

Material	ε_r (−)	σ_{cond} (Ω^{-1} m^{-1})	$t_{\text{relax}} \sim \varepsilon_r \varepsilon_o / \sigma_{\text{cond}}$ (s)
Aluminum	1	$\sim 10^{7}$	8.85×10^{-19}
Glass	4.7	$\sim 10^{-13}$	4.16×10^{2}
PTFE	2.1	$\sim 10^{-24}$	1.86×10^{13}

coupled to a 4000 QTrap® Triple-Quadrupole LC-MS system (Applied Biosystems/MDS Sciex, Foster City, CA/Toronto, Canada). The signal intensity of RDX and cocaine as a function of applied potential demonstrated an increase and leveling off, similar to the secondary droplet current measurements (see supplementary information, Figures S4 and S5[16]).[18] The inset of Figure 4 displays the normalized total ion current from these analyses as a function of the applied voltage normalized by the transition voltage, V_{es}, as was done for the deflected current measurements. As expected, the normalized mass spectrometric total ion current collapsed onto the independent deflected current measurements from Figure 4, including the asymptotic limit of emitted current for a PTFE substrate. Droplet charging and transport are imperative to analyte ionization, signal intensity, and signal-to-noise reduction for mass spectrometric detection and analysis.[18–20]

In summary, we reported the characterization of droplet charging and transport, and charge transmission for the electro-flow focusing technique as a desorption-based ambient ion source for mass spectrometric analysis. The electro-flow focusing ion source was characterized with transmitted current measurements and a scaling analysis, identifying regimes of operation and the limitations of emitted current carried by the primary droplet stream and deflected current carried by the secondary droplet stream available for analyte solvation and ionization in a desorption-style mass spectrometry analysis. The optimal voltage was determined by the device geometry, i.e., the characteristic length scale (capillary-to-orifice length) for the discharging electric field, and flow rate, i.e., higher flow rates decreased this characteristic length. Alternatively, the maximum saturation current carried by the secondary droplets was determined both by the flow rate and material properties of the interrogated substrate. This analysis identified the relationship between the electro-flow focusing ion source parameters, the substrate material properties, and the optimal applied potential, providing further insight into optimizing the transmitted current and therefore mass spectrometric response as well as enabling efficient device design and experimental operation for future investigations.

The authors thank Professor Alfonso Gañán-Calvo at the University of Seville for his informative and stimulating discussion. The authors also thank Matthew Staymates and Justin Gerber at the National Institute of Standards and Technology for their technical help in developing the current measuring LabVIEW code and helpful measurements, respectively. Certain commercial products are identified in order to adequately specify the procedure; this does not imply endorsement or recommendation by NIST, nor does it imply that such products are necessarily the best available for the purpose. The Science and Technology Directorate of the U.S. Department of Homeland Security sponsored a portion of the production of this material under Interagency Agreement IAA HSHQDC-12-X-00024 with the National Institute of Standards and Technology (NIST).

[1]A. A. Adams, P. T. Charles, J. R. Deschamps, and A. W. Kusterbeck, Anal. Chem. **83**(22), 8411 (2011).
[2]N. Gupta and R. Dahmani, Spectrochim. Acta A **56**(8), 1453 (2000).
[3]B. M. Kolakowski and Z. Mester, Analyst **132**(9), 842 (2007).
[4]M. Tabrizchi and V. Ilbeigi, J. Hazard. Mater. **176**(1–3), 692 (2010).
[5]I. Cotte-Rodríguez, Z. Takáts, N. Talaty, H. Chen, and R. G. Cooks, Anal. Chem. **77**(21), 6755 (2005).
[6]Z. Takats, I. Cotte-Rodriguez, N. Talaty, H. Chen, and R. G. Cooks, Chem. Commun. (15), 1950 (2005).
[7]G. A. Harris, A. S. Galhena, and F. M. Fernández, Anal. Chem. **83**(12), 4508 (2011).
[8]D. R. Ifa, C. Wu, Z. Ouyang, and R. G. Cooks, Analyst **135**(4), 669 (2010).
[9]D. R. Justes, N. Talaty, I. Cotte-Rodriguez, and R. G. Cooks, Chem. Commun. (21), 2142 (2007).
[10]S. Soparawalla, G. A. Salazar, E. Sokol, R. H. Perry, and R. G. Cooks, Analyst **135**(8), 1953 (2010).
[11]A. Venter, P. E. Sojka, and R. G. Cooks, Anal. Chem. **78**(24), 8549 (2006).
[12]A. M. Gañán-Calvo, Phys. Rev. Lett. **80**(2), 285 (1998).
[13]A. M. Gañán-Calvo, Phys. Rev. Lett. **98**(13), 134503 (2007).
[14]A. M. Gañán-Calvo, J. M. Lopez-Herrera, and P. Riesco-Chueca, J. Fluid. Mech. **566**, 421 (2006).
[15]J. M. Lopez-Herrera, A. M. Gañán-Calvo, and M. Perez-Saborid, J. Aerosol Sci. **30**(7), 895 (1999).
[16]See supplementary material at http://dx.doi.org/10.1063/1.4807789 for additional data and figures, including emitted, orifice discharge, and total currents; and mass spectrometric response data for cocaine and RDX.
[17]M. Volny, A. Venter, S. A. Smith, M. Pazzi, and R. G. Cooks, Analyst **133**(4), 525 (2008).
[18]T. P. Forbes, T. M. Brewer, and G. Gillen "Analytical characterization and ionization mechanisms of desorption electro-flow focusing ionization (DEFFI) mass spectrometry" (unpublished).
[19]T. P. Forbes, R. B. Dixon, D. C. Muddiman, F. L. Degertekin, and A. G. Fedorov, J. Am. Soc. Mass Spectrsc. **20**(9), 1684 (2009).
[20]R. L. Grimm and J. L. Beauchamp, J. Phys. Chem. B **109**(16), 8244 (2005).